ELSEVIER

Journal of Alloys and Compounds 311 (2000) 317–321

Journal of ALLOYS AND COMPOUNDS

www.elsevier.com/locate/jallcom

New hydride phase with a deformed FCC structure in the Ti–V–Mn solid solution–hydrogen system

Yumiko Nakamura*, Etsuo Akiba

National Institute of Materials and Chemical Research (NIMC), 1-1, Higashi, Tsukuba, Ibaraki 305-8565, Japan

Received 26 June 2000; accepted 17 July 2000

Abstract

We investigated the hydriding properties and crystal structure of a Ti–V–Mn solid solution alloy by means of *P–C* isotherm and X-ray diffraction (XRD) measurements. We found three hydride phases with a BCC, a deformed FCC and an FCC structure. The lattice constant of the deformed FCC is 0.407 nm, one axis of which is reduced by about 4%, which has not been reported so far. Its single-phase region extends over a hydrogen content between 0.8 and 1.0 H/M in absorption at 298 K. The lower plateau observed in the *P–C* isotherm due to the formation of the deformed FCC hydride phase increases the effective hydrogen capacity by decreasing the amount of hydrogen that would have remained in the alloy after the usual desorption process.

Keywords: BCC solid solution; Hydride; Deformed FCC; Hydrogen storage

1. Introduction

Metals such as Ti, V and Nb are known to form a hydride with an FCC structure, of which the hydrogen content is 2 H/M [1,2]. Some solid-solution alloys with a BCC structure containing those metal elements form a hydride with FCC structure [3,4] and Ti–V based solid-solution alloys were particularly studied as a hydrogen storage material [5–9]. Instead of the advantage of high hydrogen storage capacity, they did not seem to be suitable for practical use because of the low desorption pressure, difficulty in activation and poor kinetics.

One of the authors proposed a new concept of BCC solid solution, Laves phase related BCC solid solution in 1993 [10–12]. The Laves phase related BCC solid solutions are found in a multiphase alloy which contained a BCC phase and Laves phases. The BCC phase showed hydrogen absorption–desorption properties similar to the Laves phase, such as easiness in activation and favorable kinetics, as well as a large hydrogen storage capacity. They are distinguished from the binary Ti–V alloys which had been studied so far. Based on the concept described above, Iba et al. found that two kinds of the BCC solid-solution alloys with the compositions Ti–V–Mn and Ti–V–Cr have a large capacity as well as improved activation property and kinetics [11–13]. It should be emphasized that they showed their potential for practical use. Following their studies, Ti–V–Cr based alloys were investigated by many groups and improved in the flatness and the hysteresis in the plateau region [14–16]. However, one of the most serious problems has not been solved: 1/3 to 1/2 of the absorbed hydrogen remains in the alloy after the desorption at room temperature using a conventional vacuum pump.

Few fundamental physical properties of the Laves phase related BCC solid solutions and their hydrides have been reported so far. The crystal structure in particular affects the hydrogen absorbing properties very much, but that of the hydrides of the Laves phase related BCC solid solutions has not been reported as far as we know. More detailed studies on crystal structure and physical properties are required to understand and improve their hydriding properties.

In this study, we investigated hydriding properties and structure change of a Ti–V–Mn alloy by means of *P–C* isotherm measurements and X-ray powder diffraction.

2. Experimental

2.1. Alloys

Alloy samples were prepared by arc melting. They were

*Corresponding author.
E-mail address: yumiko@nimc.go.jp (Y. Nakamura).

0925-8388/00/$ – see front matter
PII: S0925-8388(00)01148-8

purchased from Chuo Denki Kogyo. Composition of the alloys was examined by the induction coupled plasma (ICP) method. Their average compositions obtained were $Ti_{1.00}V_{1.10\pm0.01}Mn_{0.90\pm0.01}$. The as-cast ingots were crushed into powders with particle size under 1 mm for *P–C* isotherm measurements and 30 μm for X-ray powder diffraction measurements.

2.2. P–C isotherm measurements

Powder samples were sealed into a stainless-steal container and evacuated at 353 K for 1 h. They were pressurized by 5 MPa of hydrogen gas and cooled to room temperature, followed two absorption–desorption cycles for activation. Before *P–C* isotherm measurements the samples were evacuated at 773 K. *P–C* isotherms were measured by the Sieverts method.

2.3. XRD measurements

Hydride samples were prepared by hydrogen absorption along the *P–C* isotherms. They were taken from the container into the air. The hydride phases were confirmed to be stable in air at least for a few days. Hydrogen contents of the samples were measured by a hydrogen analyzer, Leco RH-402.

X-ray powder diffraction profiles were measured using a diffractometer, Rigaku RINT-2500V. The voltage and current of the X-ray generator in this measurement were 50 kV and 200 mA. The diffraction profiles were analyzed by the Rietveld refinement program RIETAN-97beta [17–19].

3. Results

Fig. 1 shows *P–C* isotherms of $Ti_{1.0}V_{1.1}Mn_{0.9}$. It clearly shows two plateau regions in absorption. The lower plateau pressure was at around 0.01 MPa and the higher plateau pressure was at around 1 MPa at 298 K.

From the XRD profiles of the hydride samples for hydrogen contents that are indicated on the *P–C* isotherms shown in Fig. 1, we found that three kinds of hydrides were formed. Their XRD profiles are shown in Fig. 2. The first hydride (I) has a distorted BCC structure for a hydrogen content less than 0.5 H/M. Its diffraction peaks are broad and asymmetric, which indicates the structure is distorted from the original BCC. The second hydride (II) has a deformed FCC structure. Its lattice constants are 0.407 nm for two axes and 0.390 nm for the third axis. The latter is reduced by about 4% from the former. Its single-phase region is between 0.8 and 1.0 H/M in absorption at 298 K. The third and full-hydride phase (III) adopts an FCC structure, whose lattice constant is 0.432 nm. Hydrides (I) and (II) coexist in the plateau region at the lower hydrogen pressure (0.01 MPa in absorption at 298 K), and

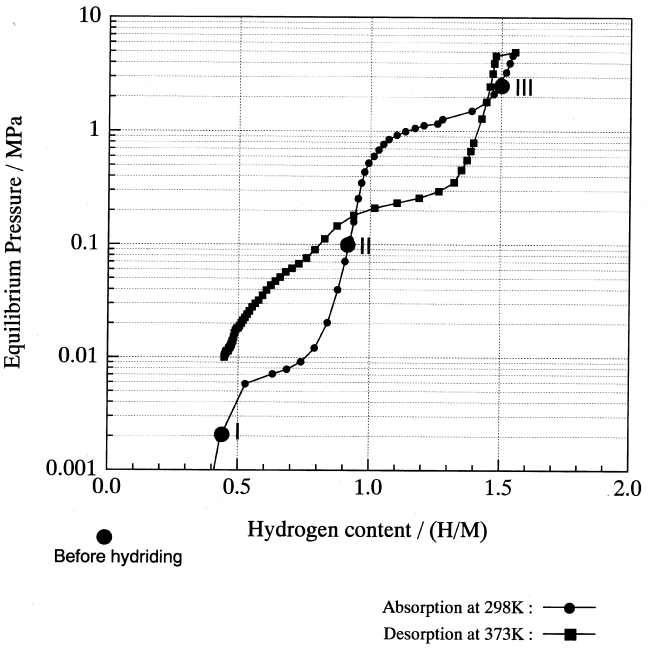

Fig. 1. *P–C* isotherms of $Ti_{1.0}V_{1.1}Mn_{0.9}$; absorption at 298 K and desorption at 373 K. Points I–III indicate the hydrogen contents of the hydrides for XRD measurements (shown in Fig. 2).

hydrides (II) and (III) coexist in the plateau region at the higher hydrogen pressure (1 MPa in absorption at 298 K). The existence of another plateau at an equilibrium pressure much lower than 0.01 MPa at room temperature, in analogy to the V–H system, was not confirmed. In the V–H system, the metal sublattice of the monohydride phase such as β-V_2H has a BCT (body-centered-tetragonal) structure with c/a ratio around 1.1 [20]. It is interesting to note that no hydride phase with a BCT structure like β-V_2H was observed in this study.

The structure of hydride (II) is a deformed FCC and is distinguished from any of the hydrides formed from BCC solid solution alloys that have ever been reported. Fig. 3 shows a result of the Rietveld analysis of the hydride (II) with a tetragonal structure model (space group: $I4/mmm$). Two impurity phases are included in the refinement. The obtained parameters are summarized in Table 1. The calculated peak positions for the hydride phase (Phase 1) match the observed diffraction peak positions and the *R*-Bragg factor, R_I, is 2.62%. However, the peak profile does not fit well, even when including an anisotropic broadening term. Also unidentified impurity phases coexist, which increases the *R*-weighted pattern R_{wp} and the 'goodness-of-fit' indicator *S*. As a result, this tetragonal model is acceptable but might need some modification for refining the structure, for example, to lower the symmetry. A purer sample would be required for further refinement. The obtained tetragonal unit cell with $a=0.288$ nm and $c=0.390$ nm corresponds to a deformed FCC unit cell with $a'=0.407$ nm and $c'=0.390$ nm as described below.

The structure change of the metal sublattice of this alloy

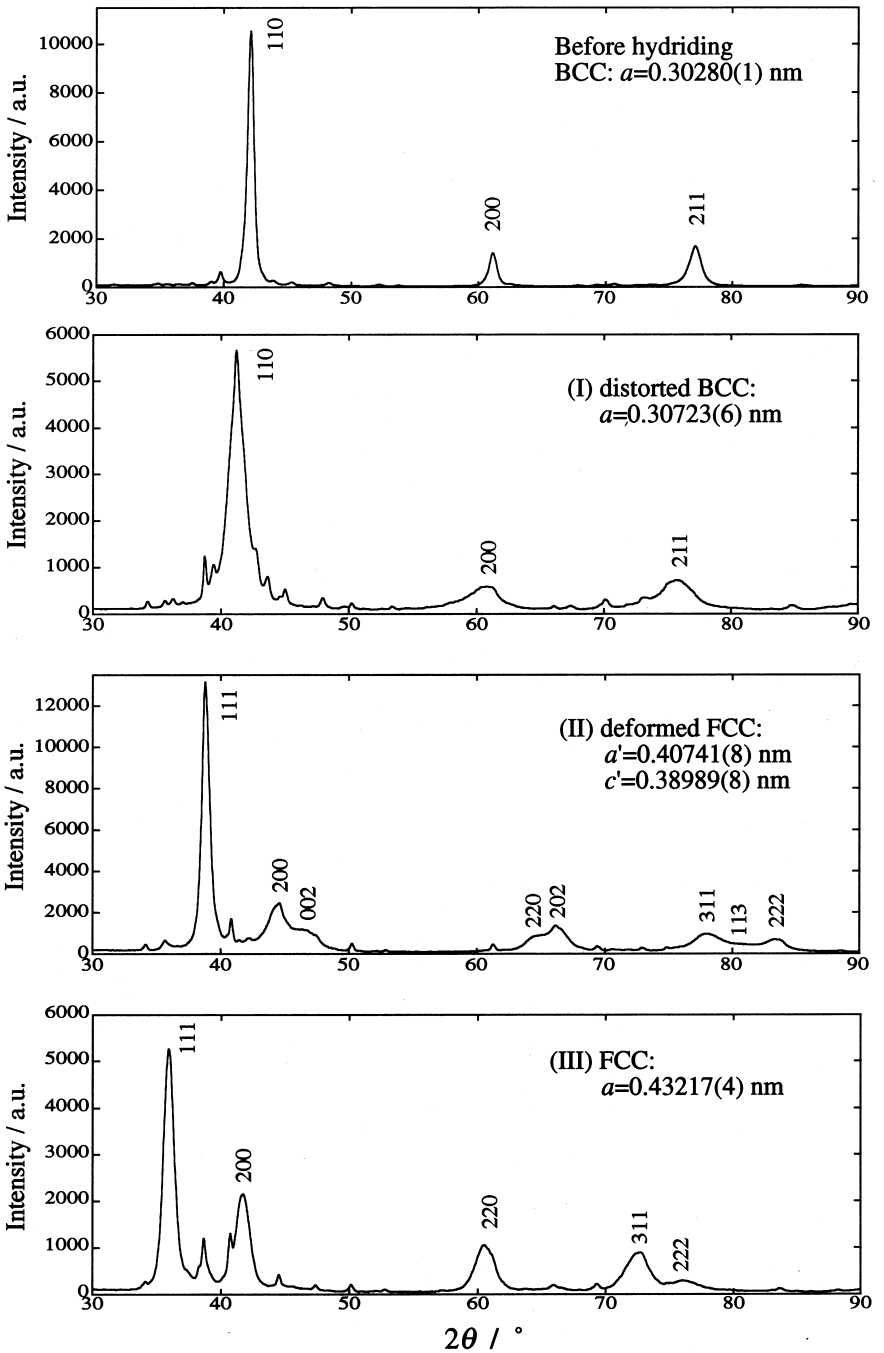

Fig. 2. XRD profiles of $Ti_{1.0}V_{1.1}Mn_{0.9}$ alloy and the three hydrides.

is illustrated in Fig. 4. Here the lattice parameters a' and c' are defined as indicated in Fig. 4. The as-cast alloy has a BCC structure. Fig. 4a shows the four BCC unit cells, where $a'=2^{1/2}a_{BCC}$, $c'=a_{BCC.}$ It changes to a little expanded and distorted structure of the hydride (I). The deformed FCC structure was formed by contraction of 6% of the a axis and expansion of about 30% of the c axis (Fig. 4b). The FCC unit cell is indicated by the shaded deformed cubic cell. Then, it is expanded by 6% in the a axis direction and 10% in the c axis direction to form the hydride (III) with an FCC structure, where $a'=c'=a_{FCC}$ (Fig. 4c). The ratio (c'/a') changes from 0.71 (BCC) to 0.96 (deformed FCC) and 1.0 (FCC). (Note: The ratio of the BCT structure reported in the V–H system is between 0.74 and 0.80 [20].)

These results reveal that the two plateaus observed in the P–C isotherm intrinsically come from the two hydrides formed from the BCC alloy. The plateau at the lower hydrogen pressure is associated with the formation of the hydride (II) with a deformed FCC structure.

The absorption–desorption P–C isotherm for the lower plateau at 353 K is shown in Fig. 5. The lower plateau has

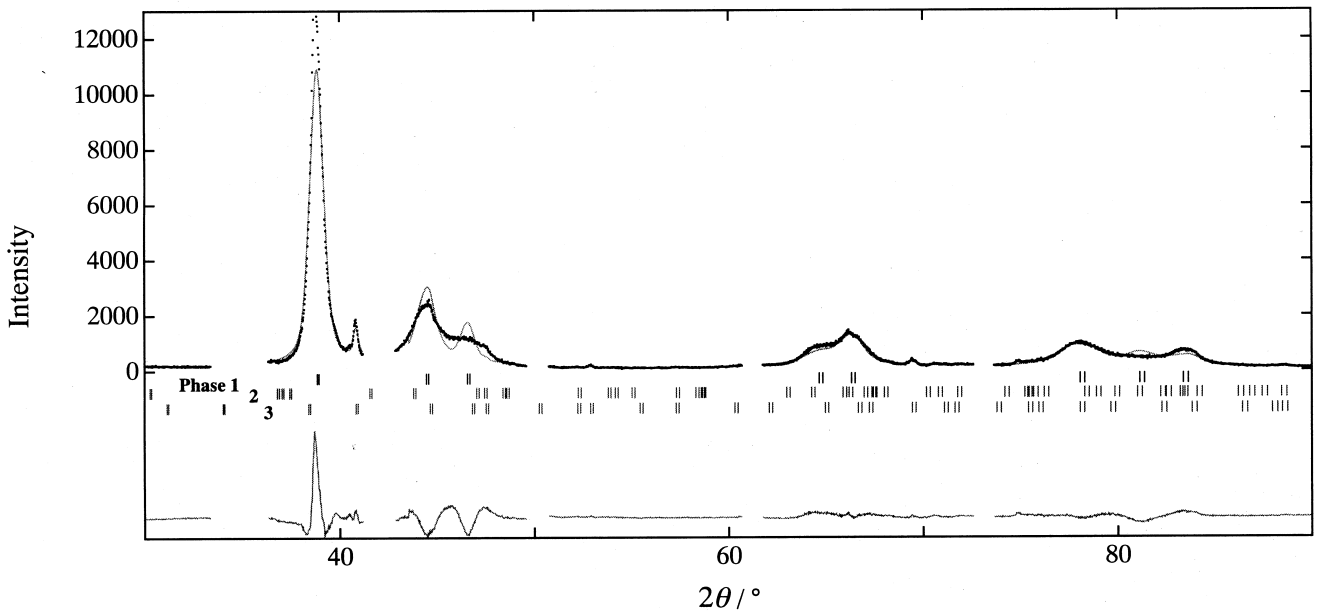

Fig. 3. XRD profile of the new Ti–V–Mn hydride analyzed by the Rietveld method with a tetragonal structure model. The space group of the structure models and obtained parameters are shown in Table 1. The gray line is the calculated intensity and the points superimposed on it are observed intensities. The tick marks below the profile indicate the positions of all allowed $K\alpha_1$ and $K\alpha_2$ peaks for the hydride phase and the impurity phases. The bottom solid line shows the difference between the calculated and observed intensities.

much smaller pressure hysteresis than the higher plateau, which suggests that the deformed FCC hydride phase is substantially different from the FCC full-hydride phase though the crystal structure and lattice constant of the metal sublattice of the two phases are similar. It may be considered that occupation of hydrogen atoms in the interstitial sites is different in the two phases. A detailed investigation of the hydrogen occupation is underway by neutron diffraction and incoherent inelastic neutron scattering studies.

The lower plateau due to the formation of the deformed FCC hydride phase leads to an increase of effective hydrogen capacity by decreasing the amount of hydrogen remaining in the alloy after desorption. The authors expect that in BCC solid solution alloys with various compositions the possibility might exist to form an intermediate hydride phase with a stability suitable for reversible hydrogen storage.

4. Conclusions

We investigated the hydriding property and crystal structure of a Ti–V–Mn solid solution alloy and found a new hydride phase. Its P–C isotherms showed two plateau regions and three single-phase regions between 0.01 MPa and 5 MPa around room temperature.

The crystal structures of the three hydride phases are BCC, deformed FCC and FCC. The deformed FCC is the new hydride phase, of which the lattice constant is 0.407 nm and one axis of which is reduced by about 4%. Its single-phase region corresponds to a hydrogen content between 0.8 and 1.0 H/M in absorption at 298 K.

The plateau due to the formation of the new hydride phase increases the effective hydrogen capacity by decreasing the amount of hydrogen remaining in the alloy after the desorption process. The BCC solid solution alloys which form an intermediate hydride phase such as the

Table 1
Structural parameters of the Ti–V–Mn hydride phase (II) obtained from the XRD profile by the Rietveld method[a]

Phase	a (nm)	c (nm)	Fraction (%)	R_I (%)
1. Ti–V–Mn hydride (II) deformed FCC $I4/mmm$ (No. 139)	0.28808(6)	0.38989(8)	93.2	2.62
2. C14 Laves phase $P6_3/mmc$ (No. 194)	0. 590(4)	0. 827(6)	3.5	2.83
3. Zr_3V_3O or Ti_4Fe_2O type $Fd\bar{3}m$ (No. 227)	1.1475(5)		3.3	3.35

[a] $R_{wp} = 16.68\%$, $S = 4.31$.

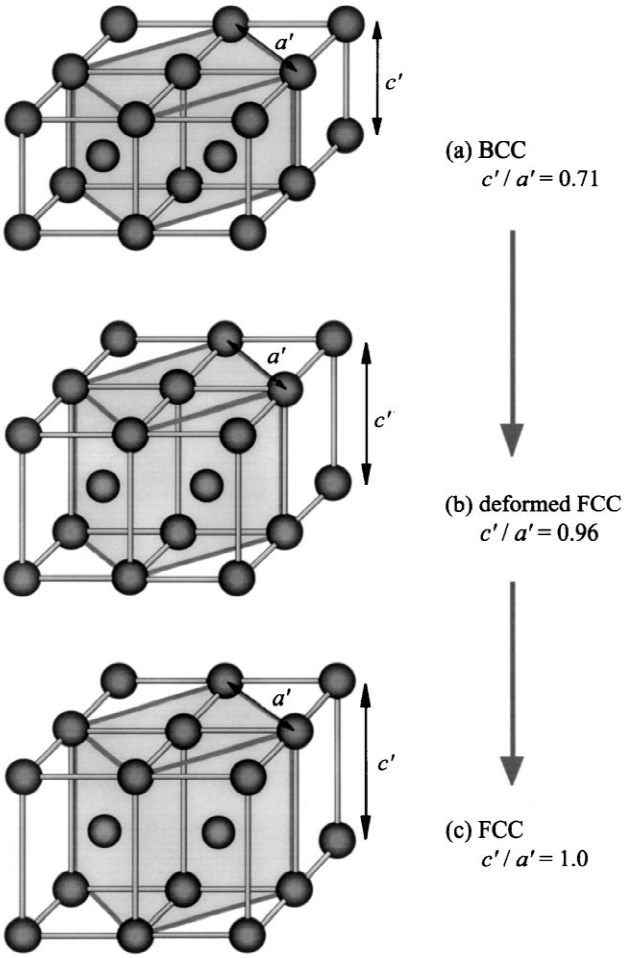

Fig. 4. Change of the crystal structure of the metal lattice from the BCC alloy to the deformed FCC hydride and the FCC full-hydride.

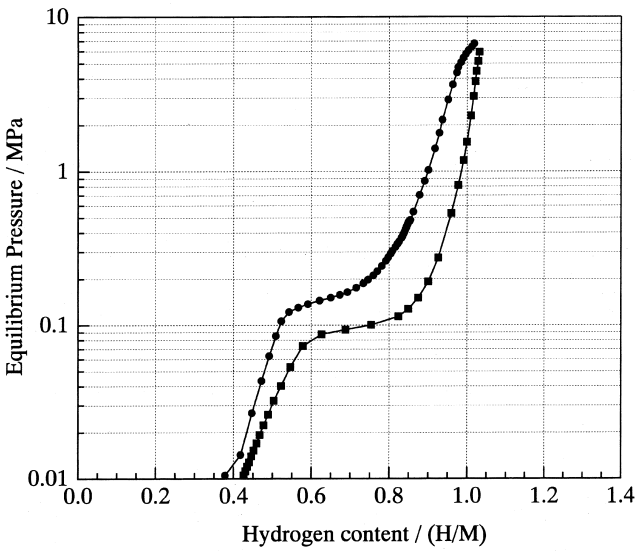

Fig. 5. Absorption and desorption P–C isotherms of $Ti_{1.0}V_{1.1}Mn_{0.9}$ for the lower plateau measured at 353 K.

Ti–V–Mn alloy are potential materials for on-board hydrogen storage.

Acknowledgements

Part of this work was supported by the WE-NET project by the New Energy and Industrial Technology Development Organization (NEDO) under the Ministry of International Trade and Industry, and a Giant-in-Aid for Scientific Research on Priority Area A of New Protium Function in Sub-Nano Lattice Matters from the Ministry of Education, Science, Sports and Culture, Japan.

References

[1] T. Schober, H. Wenzl, Hydrogen in Metals II, in: G. Alefeld, J. Völkl (Eds.), Topics in Applied Physics, Vol. 29, Springer, Berlin, Heidelberg, 1978, Chapter 1.
[2] J.J. Reilly, R.H. Wiswall Jr., Inorg. Chem. 9 (1970) 1678.
[3] S. Hayashi, K. Hayamizu, J. Less-Common Met. 161 (1990) 61.
[4] T. Hagi, Y. Sato, M. Yasuda, K. Tanaka, Trans. Japan Inst. Met. 28 (3) (1987) 198.
[5] S. Ono, K. Nomura, Y. Ikeda, J. Less-Common Met. 72 (1980) 159.
[6] J.F. Lynch, A.J. Mealand, G.G. Libowitz, J. Less-Common Met. 103 (1984) 117.
[7] A.J. Mealand, G.G. Libowitz, J.F. Lynch, J. Less-Common Met. 104 (1984) 361.
[8] G.G. Libowitz, A.J. Mealand, J. Less-Common Met. 131 (1987) 275.
[9] T. Kabutomori, H. Takeda, Y. Wakisaka, K. Ohnishi, J. Alloys Compd. 231 (1995) 528.
[10] J. Huot, E. Akiba, H. Iba, J. Alloys Compd. 228 (1995) 181.
[11] H. Iba, E. Akiba, J. Alloys Compd. 231 (1995) 508.
[12] E. Akiba, H. Iba, Intermetallics 6 (1998) 461.
[13] H. Iba, E. Akiba, J. Alloys Compd. 253–254 (1997) 21.
[14] Y. Tominaga, S. Nishimura, T. Amemiya, T. Fuda, T. Tamura, T. Kuriiwa, A. Kamegawa, M. Okada, Mater. Trans., JIM 41 (5) (2000) 617.
[15] S.-W. Cho, C.-S. Han, C.-N. Park, E. Akiba, J. Alloys Compd. 288 (1999) 294.
[16] H. Arashima, H. Tohgo, H. Itoh, T. Kabutomori, in: Abstracts of fall meeting of the Japan Institute of Metals, 1999, p. 289, (in Japanese).
[17] F. Izumi, Rigaku-Denki J 34 (1) (1996) 18, (in Japanese).
[18] F. Izumi, http://www.nirim.go.jp/~izumi/
[19] F. Izumi, in: R.A. Young (Ed.), The Rietveld Method, International Union of Crystallography, Oxford University Press, 1993, Chapter 13.
[20] H. Asano, Y. Abe, M. Hirabayashi, Acta Met. 24 (1976) 95.